International Journal of Microwave and Wireless Technologies

cambridge.org/mrf

Eight-port multiband MIMO antenna design with high isolation for 5G smartphones

A. Vincy Lumina, Sangeetha Manoharan and Sachin Kumar

Department of Electronics and Communication Engineering, SRM Institute of Science and Technology, Kattankulathur, India

Research Paper

Cite this article: Lumina AV, Manoharan S, Kumar S (2024) Eight-port multiband MIMO antenna design with high isolation for 5G smartphones. *International Journal of Microwave and Wireless Technologies* **16**(8), 1316–1330. https://doi.org/10.1017/S1759078724000849

Received: 19 February 2024
Revised: 16 August 2024
Accepted: 18 August 2024

Keywords:
hand phantom; isolation; meandered radiator; multiband antenna; smartphones

Corresponding author:
Sangeetha Manoharan;
Email: sangeetm@srmist.edu.in

Abstract

This paper presents the design and analysis of a compact eight-port multiband multiple-input–multiple-output (MIMO) antenna for 5G smartphones. The proposed antenna structure is designed using meandering elements, as radiator, on the FR4 substrate of 150 × 80 × 0.8 mm with loss tangent (tan δ) of 0.02 and relative permittivity (ε_r) of 4.4. The proposed antenna resonates at 2.4, 3.5, and 5.5 GHz, and it covers the bandwidth of 2%, 6.28%, and 2.53%, respectively. The measured results provide an omnidirectional radiation pattern with 58%–78% of efficiency in all operating bands. The eight-port multiband MIMO design provides a high isolation of 17.5 dB, envelope correlation coefficient < 0.04, diversity gain of 9.98 dB, total active reflection coefficient < -10 dB, and channel capacity loss of <0.25 bits/s/Hz. Also, the hand phantom is designed to analyze the reflection coefficients and efficiency of the proposed antenna.

Introduction

Multiple-input–multiple-output (MIMO) systems with frequency diversity are the optimal choice for improved coverage and ultra-fast transmission rates [1–3]. The authors of reference [4] presented a MIMO antenna with a square patch and a modified complementary electric inductive capacitive resonator designed on the FR4 substrate, resonating at 2.45, 3.5, and 4.4 GHz. This design features a peak isolation of 47 dB due to hexagonal-shaped split ring resonators (SRRs) in the ground plane. In reference [5], the authors proposed a 20 × 20 mm MIMO antenna on FR4 substrate that produces triple bands at 1.8, 2.4, and 3.5 GHz with the help of meta-resonator to achieve gain of 1.9, 1.75, and 1.52 dBi, respectively. The references [4, 5] present the different techniques used for multiband operation, reduced antenna size, and frequency diversity. The MIMO antenna has a challenge of coupling among the resonating elements, which can be encountered with the help of defected ground surface, parasitic reflectors and neutralization lines. In reference [6], a single band MIMO antenna of 26.43 × 38.25 mm, with four ports designed on FR4 substrate, is used for 4.4–5 GHz band, wherein the radiators are orthogonally placed to produce an isolation of 25 dB, reducing mutual coupling and obtain a peak gain of 2.8 dBi used for 5G applications. MIMO antenna system that covers 3.4–3.6 GHz with H-shaped resonators, of size of 20 × 20 mm, in orthogonal arrangement used for 5G applications is reported in reference [7]. This offers a bandwidth of 200 MHz and isolation of >12 dB with FR4 substrate of 0.8 mm thickness. A quad-port MIMO antenna of 45 × 45 mm with FR4 as a substrate is proposed in reference [8], which consists of a circular stub in the ground to achieve ultra-wideband range of 3.1–11 GHz for Wi-MAX, WLAN, and C-band applications. A four-port antenna of 60 × 60 mm with FR4 substrate is presented in reference [9], in which two arms with an open slot ground plane is used for bandwidth enhancement that operates at 3.4–3.8 GHz. The single band and low-level isolation limit its practical application.

In reference [10], the authors proposed a MIMO antenna of 46 × 21 mm, designed on the FR4 substrate of 1.6 mm thickness, with a circular-shaped SRR on top and a defected ground at the bottom to produce dual bands that provide linear polarization and circular polarization in each band. The gain of the antenna is 3.25 and 3.4 dBi in 3.4–3.6 GHz and 4–8 GHz bands, respectively, with more than 15 dB isolation used for 5G and C band applications. In reference [11], the authors proposed a four-port SRR induced inverted L-monopole antenna on the FR4 substrate of 40 × 40 mm. The lower frequency mode merges with SRR to obtain a wider bandwidth of 35.21% and gain of 4 dBi at 2.9 GHz for 5G applications. It also presents MIMO parameters like envelope correlation coefficient (ECC), total active reflection coefficient (TARC), channel capacity loss (CCL) with acceptable value limits. A MIMO antenna of 35 × 28 mm designed on FR4 substrate is presented in reference [12] to produce dual-band operation, with the help of closely spaced U-slots, at 2.6 and 3.6 GHz. It has parasitic structures of C-shape to reduce mutual coupling in the operating bands, where the isolation obtained is of 13 and 10 dB at resonant frequencies. Antenna configurations proposed in references [10–12] have larger substrate area, complicated design, and poor performance.

In reference [13], a dual-band MIMO antenna with FR4 substrate is reported with dimensions of 7 × 6.2 mm for 5G mobile applications, and use a parasitic stub method to cover 3.4–3.93 GHz and 4.5–5.3 GHz with isolation of 10 dB, efficiency > 50%, and ECC < 0.23. In reference [14], a T-shaped monopole MIMO antenna with FR4 substrate is presented for 5G mobile applications. The antenna has dimensions of 21.8 × 7 mm, produces an isolation of 12.8 dB, ECC lower than 0.18 and efficiencies of 71% and 68% in 3.3–3.6 GHz and 4.4–5 GHz bands, respectively. In reference [15], a four-port low profile MIMO antenna is presented for 5G mobile applications mounted on FR4 substrate with wideband shared-radiator. The antenna with dimensions of 19 × 19 mm has four corner-cut patches with grounded square analyzed through characteristic mode analysis, and it produces isolation of 10 dB and efficiencies of 40.3%–48.5% in the frequency range of 4.4–5 GHz. Another eight-element MIMO antenna for 5G mobile applications is presented in reference [16], which resonates at 3.1–3.7 GHz, 4.47–4.91 GHz, and 5.5–6.0 GHz. The antenna dimensions are 19 × 7 mm and produces spatial diversity characteristics with efficiencies of 62% and 78%, isolation greater than 16 dB and 5.8 dBi of peak gain. In reference [17], a mobile phone antenna is designed of dimensions of 46 × 1 mm with dual feed shared radiator on FR4 substrate to cover Global Positioning System (GPS) and Long Term Evolution (LTE) bands at 1172–1205 MHz and 1410–2790 MHz with improved isolation of 14.8 dB and efficiencies from 52.5%–63.9%. In reference [18], an 8 × 8 MIMO antenna with dimensions of 3 × 21.5 mm is presented, which has isolation greater than 17.5 dB with the help of balanced open-slot design between the ports. The antenna is designed for 5G mobile applications, and it has an efficiency of >62% and ECC < 0.05. The designs in the above references are used in miniaturizing MIMO antennas in smartphones. However, these designs cannot reduce the size of antenna further with a greater number of antenna elements. Therefore, designing a miniaturized antenna with larger number of antenna elements, which can be used to develop a MIMO antenna for smartphones, is still a challenge.

In this paper, the designed antenna is a compact multiband MIMO configuration for 5G smartphones with improved isolation. The proposed antenna resonates at 2.4, 3.5, and 5.5 GHz with omnidirectional radiation patterns. The objectives of the proposed eight-port multiband MIMO antenna are:

- To achieve the frequency bands that resonates at 2.4, 3.5, and 5.5 GHz without any parasitic elements.
- To obtain isolation of >17.5 dB between the antennas.
- To study the antenna characteristics on a hand phantom model to check its performance such as S_{11}, total efficiency, and ECC.

This work is organized as follows: The "Design of an eight-port multiband MIMO antenna" section elaborates the design of an eight-port multiband MIMO antenna, the "Analysis of the eight-port multiband MIMO antenna" section describes the analysis of the proposed MIMO antenna, the "Performance analysis using hand-phantom mode" section analyzes the efficiency, ECC, and S-parameters using hand phantom model, and the "Conclusion" section describes the conclusion of the work.

Design of an eight-port multiband MIMO antenna

The proposed antenna has meandering elements that are etched on 150 × 80 mm FR4 substrate ($\varepsilon_r = 4.4$ and $\tan\delta = 0.02$) with 0.8 mm of thickness, and the single antenna has a size of 16.5 × 8.5 mm ($0.132\lambda_0 \times 0.068\lambda_0$, where λ_0 is the free space wavelength calculated at the lowest frequency). The antenna has eight elements (ANT 1–8), in which, antenna 1 and antenna 5 are placed in horizontal direction along the short edges, and antennas 2–4 and 6–8 are placed in vertical direction along the long edges.

The expanded layout of the proposed antenna is indicated in Fig. 1. The proposed eight-port multiband MIMO antenna is simulated using CST Microwave Studio Suite software, and Table 1 shows the dimensions of the proposed eight-port multiband MIMO antenna. It has an inverted E-shaped slot radiator on the ground plane, which has two open ends. In the radiator, there is a branch slot on the either of the open-ended vertical slot, and a microstrip line is used in the slot radiator to feed it.

Every antenna element is designed to resonate at 2.4, 3.5, and 5.5 GHz using equations (1–3), respectively.

$$f_{3.5\,\mathrm{GHz}} = \frac{0.61 * c}{\begin{array}{c}(L_1 + W_1 + L_3 + W_3 + L_4 + W_4 + L_5 \\ + W_5 + L_6 + W_6 + L_7 + W_7) * \sqrt{\frac{\varepsilon_r + 1}{2}}\end{array}} \tag{1}$$

$$f_{2.4\,\mathrm{GHz}} = \frac{0.56 * c}{(L_1 + W_1 + d) * \sqrt{\frac{\varepsilon_r + 1}{2}}} \tag{2}$$

$$f_{5.5\,\mathrm{GHz}} = \frac{0.623 * c}{(L_1 + W_1 + L_3 + W_2) * \sqrt{\frac{\varepsilon_r + 1}{2}}} \tag{3}$$

Design novelty

The proposed MIMO antenna composed of eight resonators with an ordinary ground plane and no decoupling element among the radiators is used to improve isolation.

- The antenna elements 1 and 5, 2 and 8, 3 and 7, and 4 and 6 are mirror images of each other so the coupling current vectors are in the opposite direction. Due to this mirror-image arrangement of the resonating elements, the proposed MIMO antenna achieves polarization diversity thereby providing high isolation without the need for an additional decoupling mechanism.
- The proposed antenna design achieves multiband by using an E-shaped slot in the ground plane, and the ground plane disrupts unwanted current paths, reducing coupling between antenna elements.
- The meandering of the conductive patch reduces the physical dimensions of the antenna while maintaining the desired electrical length. This allows for a more compact design, which is beneficial in space-constrained applications like mobile devices.
- Despite the compact size, the proposed antenna elements can achieve good radiation efficiency ensuring strong signal transmission and reception, particularly in low-power applications.
- The antenna element can be tailored to meet specific design requirements, such as desired resonant frequency, bandwidth, and radiation pattern. This flexibility makes it adaptable to integrate into printed circuit boards (PCBs) and other

https://doi.org/10.1017/S1759078724000849 Published online by Cambridge University Press

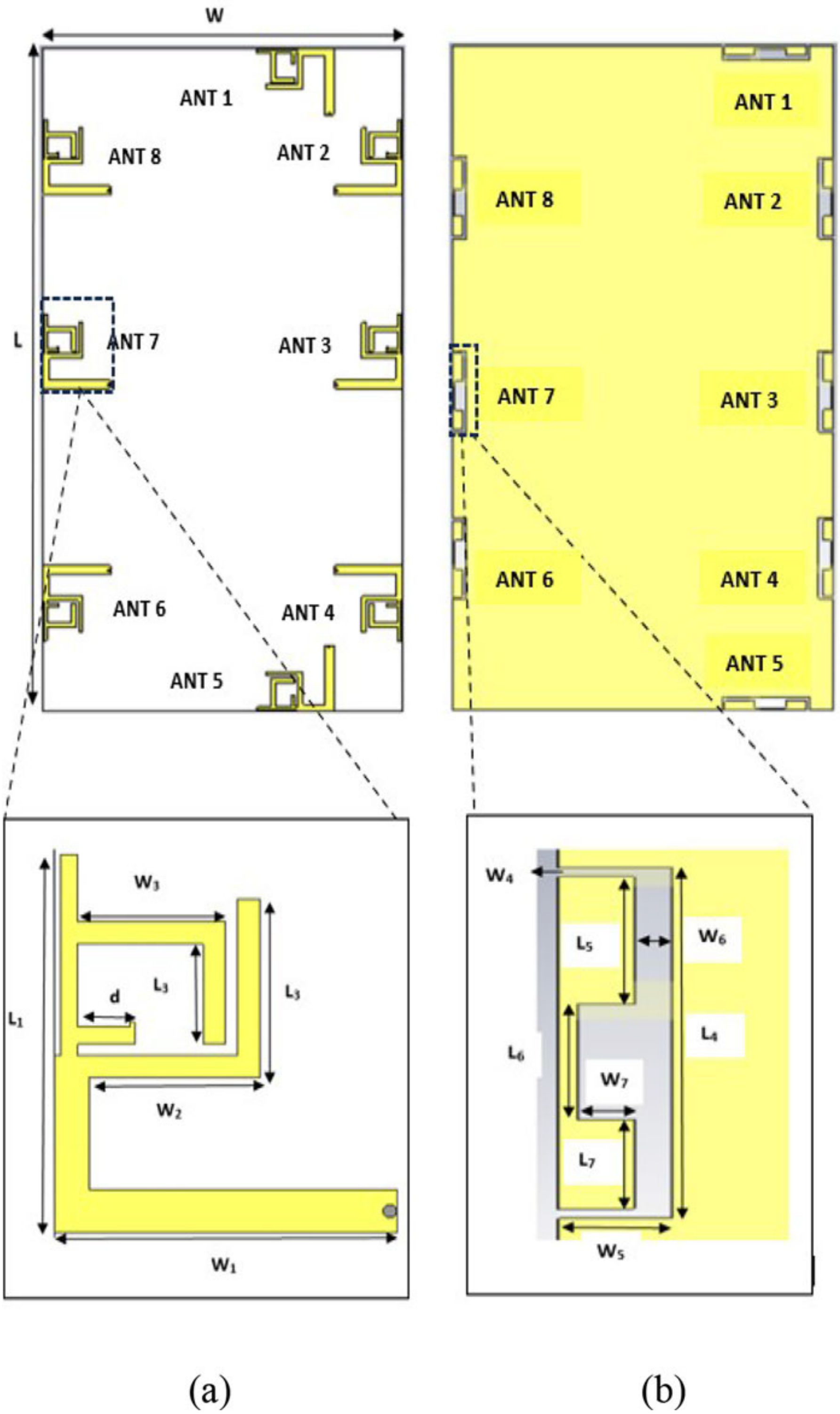

(a) (b)

Figure 1. (a), (b). Top and bottom view of the proposed multiband MIMO antenna.

electronic devices, facilitating the design of compact and integrated wireless gadgets/devices.

- Mirrored antenna elements in the proposed antenna can help to achieve better isolation between individual antenna elements, improving the performance of MIMO algorithms that rely on separating the multiple transmitted and received signals.
- With reduced correlation, the proposed MIMO antenna can achieve higher diversity and multiplexing gains, resulting in better performance metrics such as signal-to-noise ratio.
- The planar structure of the proposed meandered line antenna contributes to a low-profile design, which is aesthetically pleasing and practical for embedding in thin devices like smartphones and tablets.

https://doi.org/10.1017/S1759078724000849 Published online by Cambridge University Press

Table 1. Dimensions of the proposed eight-port multiband MIMO antenna

Parameters	L	W	L_1	W_1	L_2	W_2	L_3	W_3	d
Dimensions (mm)	150	80	16.5	15	7	7.5	5.5	7.5	2.5
Parameters	L_4	W_4	L_5	W_5	L_6	W_6	L_7	W_7	
Dimensions (mm)	18.5	0.5	7.1	3.5	6.7	1	4.7	1.5	

Evolution stages of the proposed multiband single antenna

The evolution stages of the proposed antenna are shown in Fig. 2. The antenna has a meandering element over the feed lines to resonate at 3.5 GHz, as shown in Fig. 2(a). To cover the 5.5 GHz frequency for Wi-MAX application, an additional meandering element is introduced internally, as shown in Fig. 2(b). Finally, to obtain the WLAN operating frequency at 2.4 GHz, external meandering element is incorporated in the antenna, as shown in Fig. 2(c). The S_{11} of the three stages are given in Fig. 3.

Eight-port multiband MIMO antenna placement

The placement of the radiating elements for an eight-port antenna is decided by placing them in different positions and analyzing their S-parameters.

Case 1

In this case, the position of the radiating elements 1 and 5 is reversed, as shown in Fig. 4(a), so that the open ends of the two antennas (ANT 1 and ANT 5) are very close to the PCB corners. Due to this, the eight-port arrangement for the multiband MIMO antenna does not resonate at 3.5 GHz frequency band. Also, the isolation between antennas 1 and 2 and antennas 4 and 5 (S_{21} and S_{54}) is 13.5–17.5 dB, as shown in Fig. 4(b).

Case 2

In this case, the position of the radiating elements 2, 4, 6, and 8 is reversed, as shown in Fig. 5(a). The isolation between the antennas is reduced to 12 dB, as shown in Fig. 5(b). As the open ends of the radiating elements are facing each other, due to the lesser distance between both the antennas, an undesirable isolation is obtained.

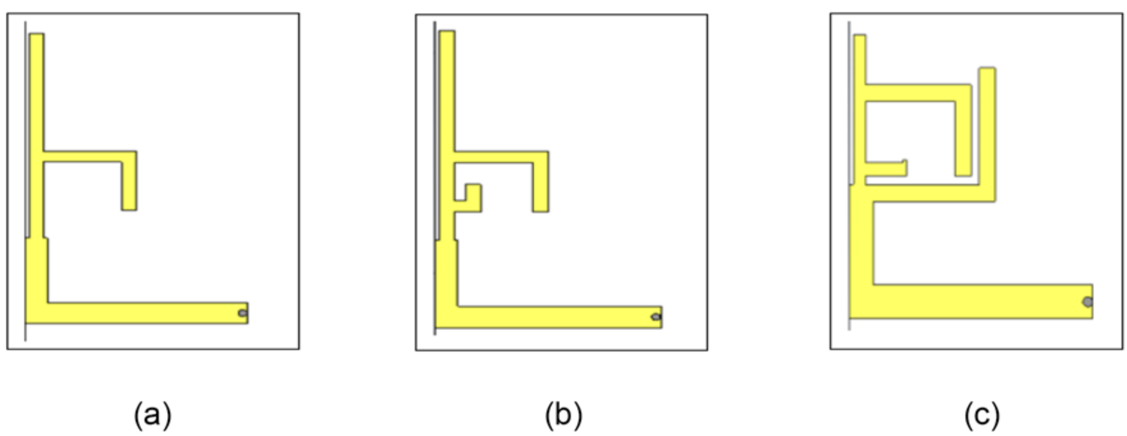

Figure 2. (a–c). Evolution stages of the proposed multiband single antenna.

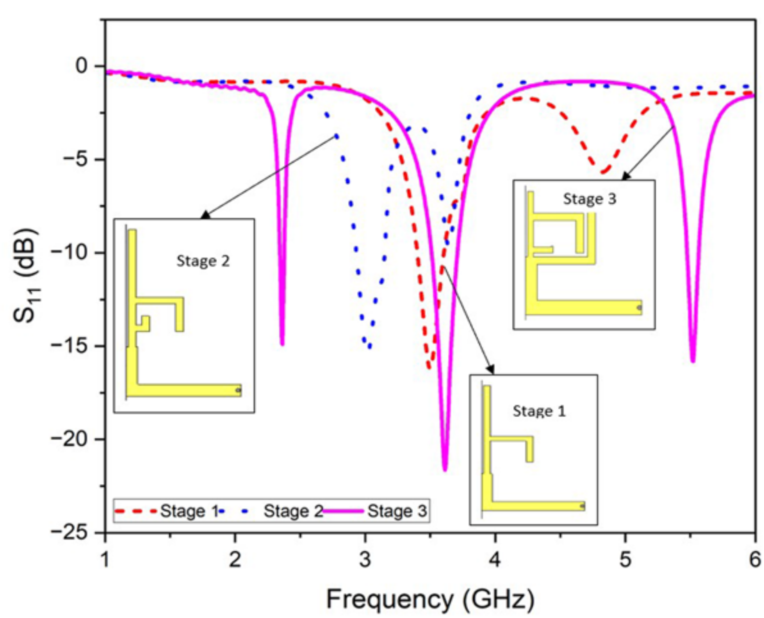

Figure 3. S_{11} of the evolution stages of the proposed multiband single antenna.

https://doi.org/10.1017/S1759078724000849 Published online by Cambridge University Press

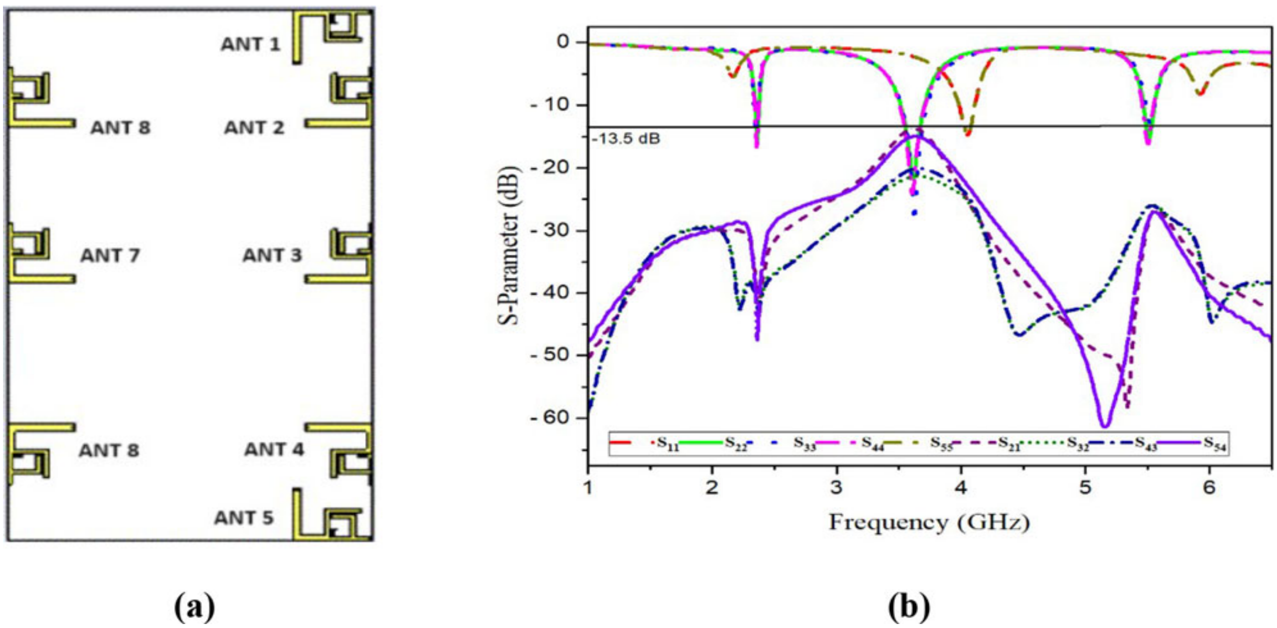

Figure 4. (a), (b). Design and its S-parameters of Case 1.

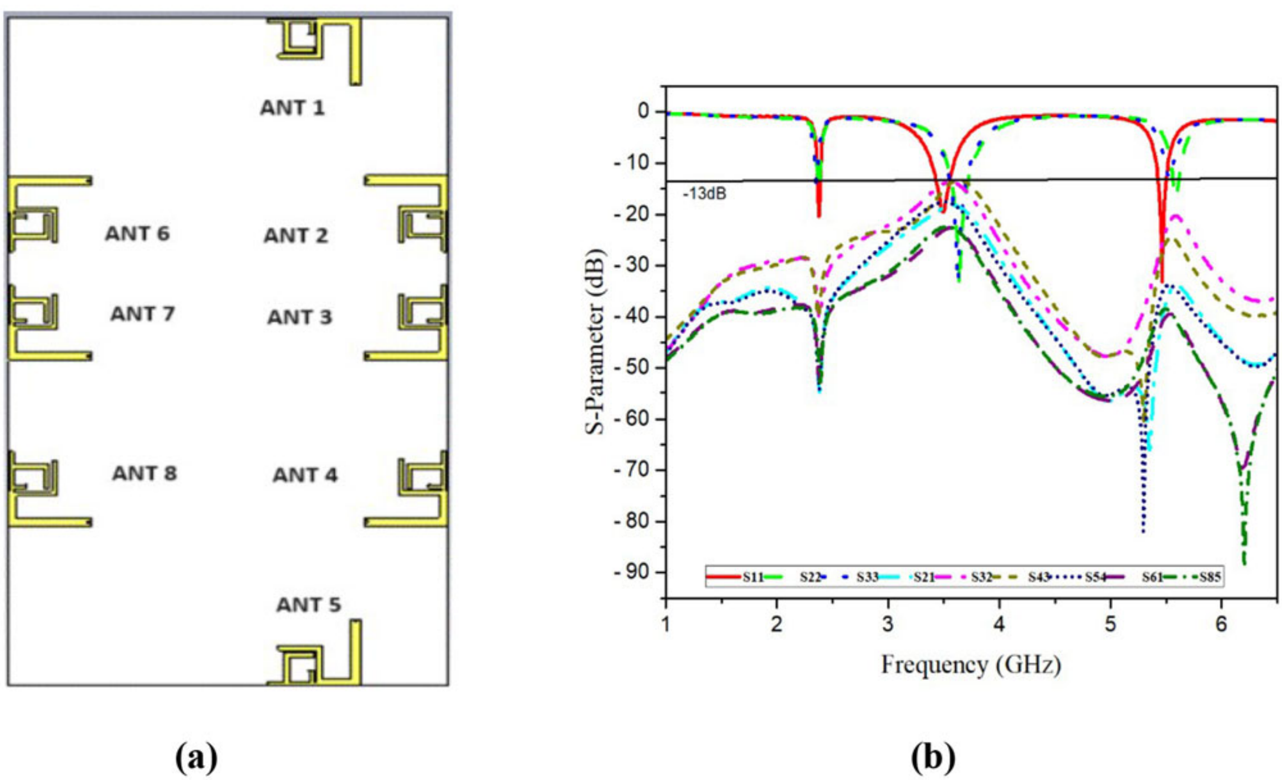

Figure 5. (a), (b). Design and its S-parameters of Case 2.

It is observed that the two antennas that are adjacently placed causes poor isolation than the antennas placed away from each other. Therefore, the two face to face adjacent radiating elements should be placed away from each other (as in antennas 1 and 6 and antennas 5 and 8) to obtain enhanced isolation.

Case 3

This case shows the orthogonal arrangements of the radiating elements in which they are placed perpendicularly, as shown in Fig. 6(a). The orthogonal antenna polarization does not cover the resonating frequencies (3.5 and 5.5 GHz) and provides deteriorated

https://doi.org/10.1017/S1759078724000849 Published online by Cambridge University Press

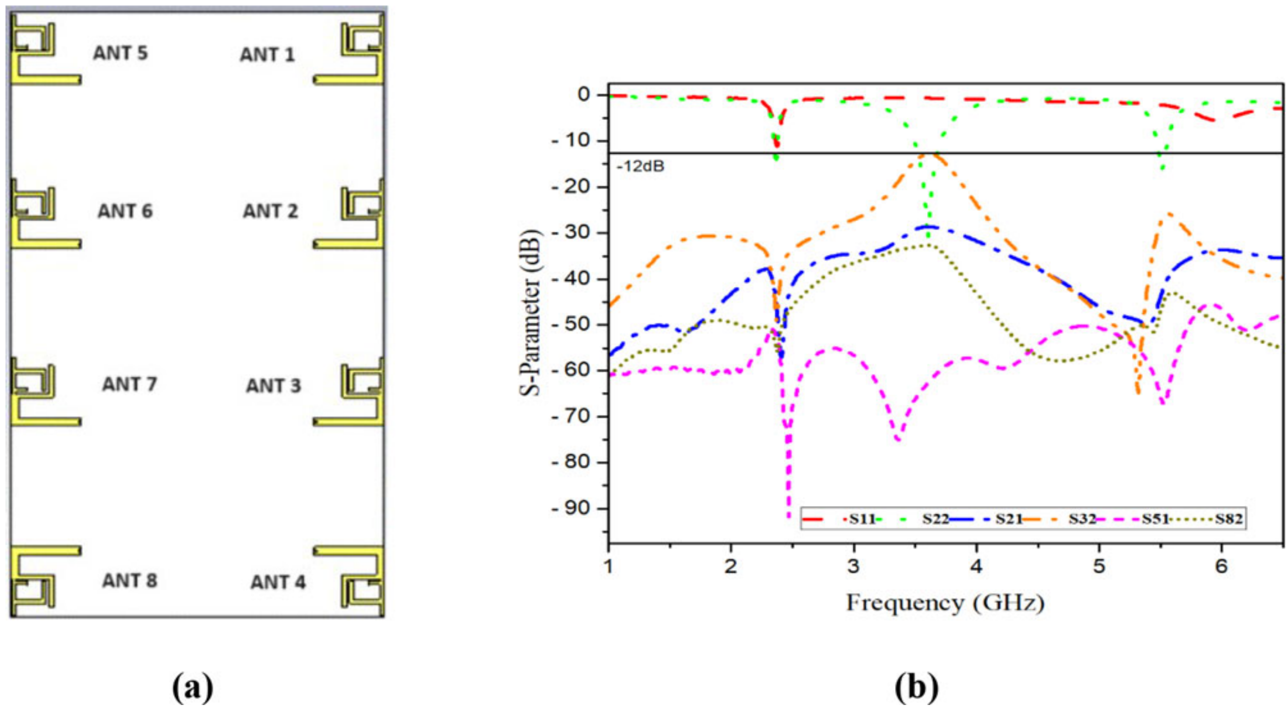

Figure 6. (a), (b). Design and its S-parameters of Case 3.

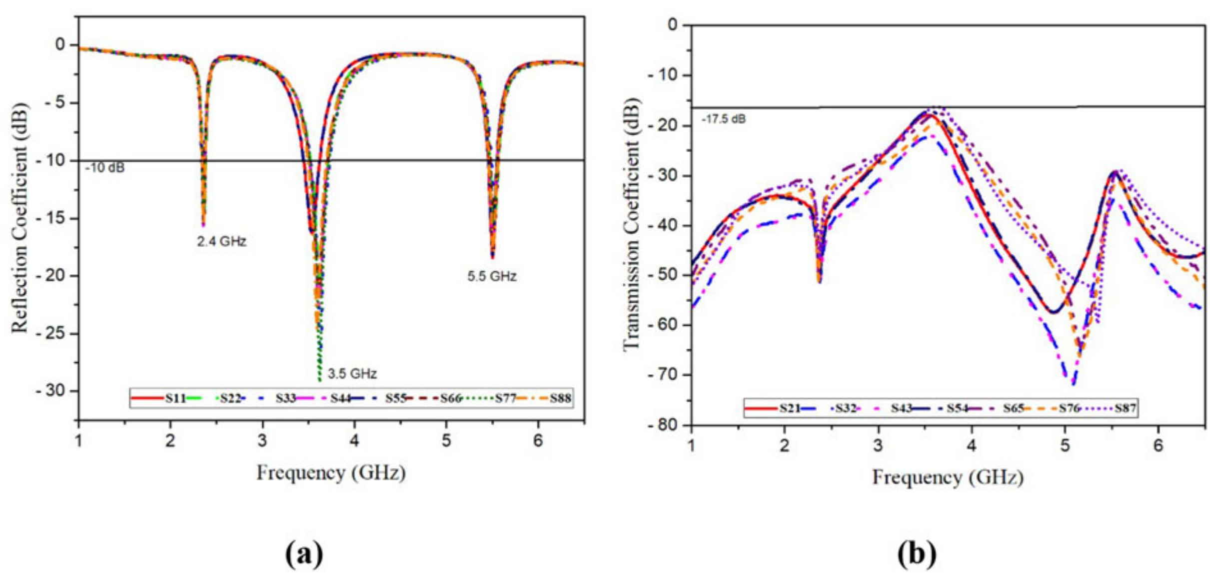

Figure 7. (a), (b). Simulated S-parameters of the eight-port multiband MIMO antenna.

isolation, as shown in Fig. 6(b). This case cannot yield good antenna performance.

Case 4

To improve the isolation between the antenna elements, the antennas 1 and 5 are placed away from the nearby antennas 2 and 4, as shown in Fig. 1. This produces the bandwidth of 2%, 6.28%, and 2.53% at 2.4, 3.5, and 5.5 GHz, respectively. From Fig. 7, it is observed that the proposed eight-port multiband MIMO antenna operates at 2.4, 3.5, and 5.5 GHz with an isolation of 17.5 dB.

Current distribution

The two antennas connecting at the common null are in reverse direction. As there is a less current distribution in the ground, a high isolation level is achieved. Also, as stipulated by the current distribution in Fig. 8, if the antennas are in perpendicular direction, the x-axis and y-axis generate orthogonal polarizations, resulting in low isolation.

The antenna proposed in this work resonates at 2.4, 3.5, and 5.5 GHz, making it suitable for 5G smartphones while having smaller dimensions. The fabrication process is simple

https://doi.org/10.1017/S1759078724000849 Published online by Cambridge University Press

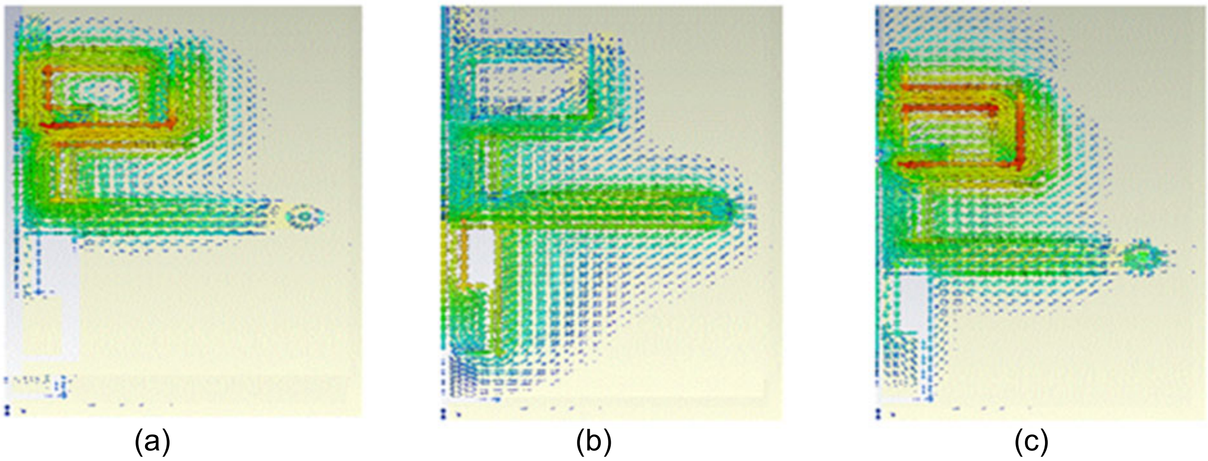

Figure 8. (a–c) Surface current distribution at 2.4, 3.5, and 5.5 GHz.

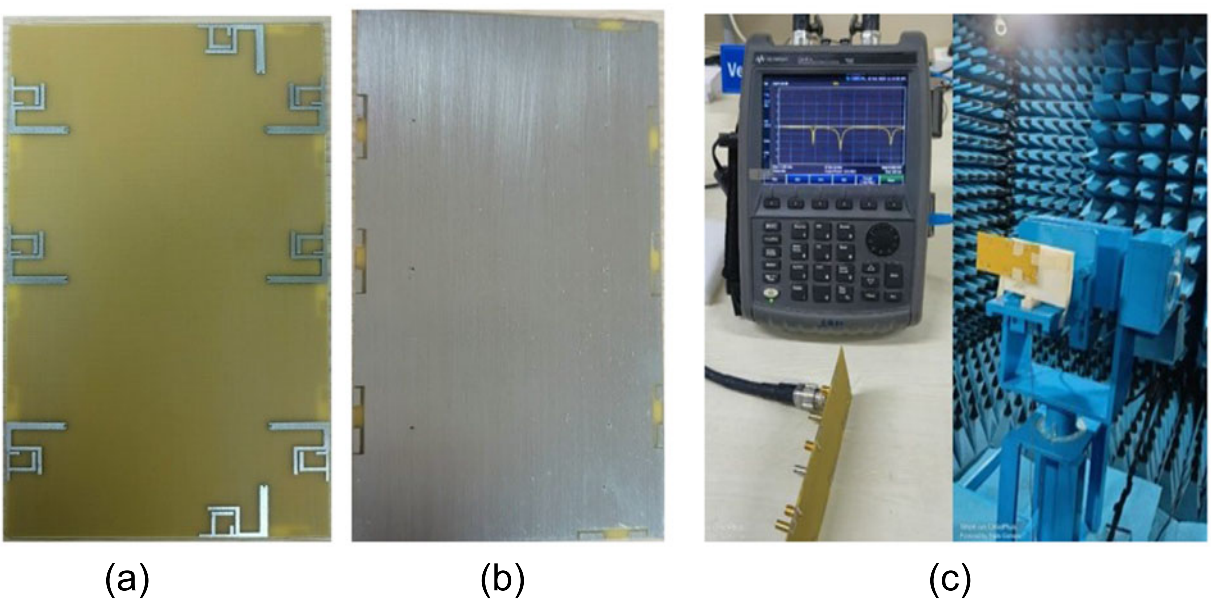

Figure 9. (a–c). Prototype of the proposed MIMO antenna.

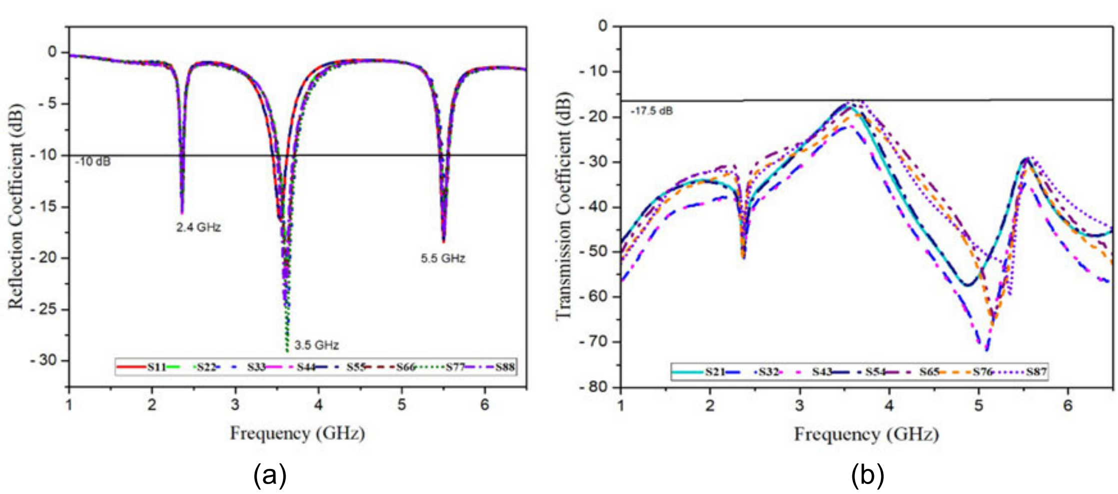

Figure 10. (a), (b). Measured S-parameters of the proposed MIMO antenna.

https://doi.org/10.1017/S1759078724000849 Published online by Cambridge University Press

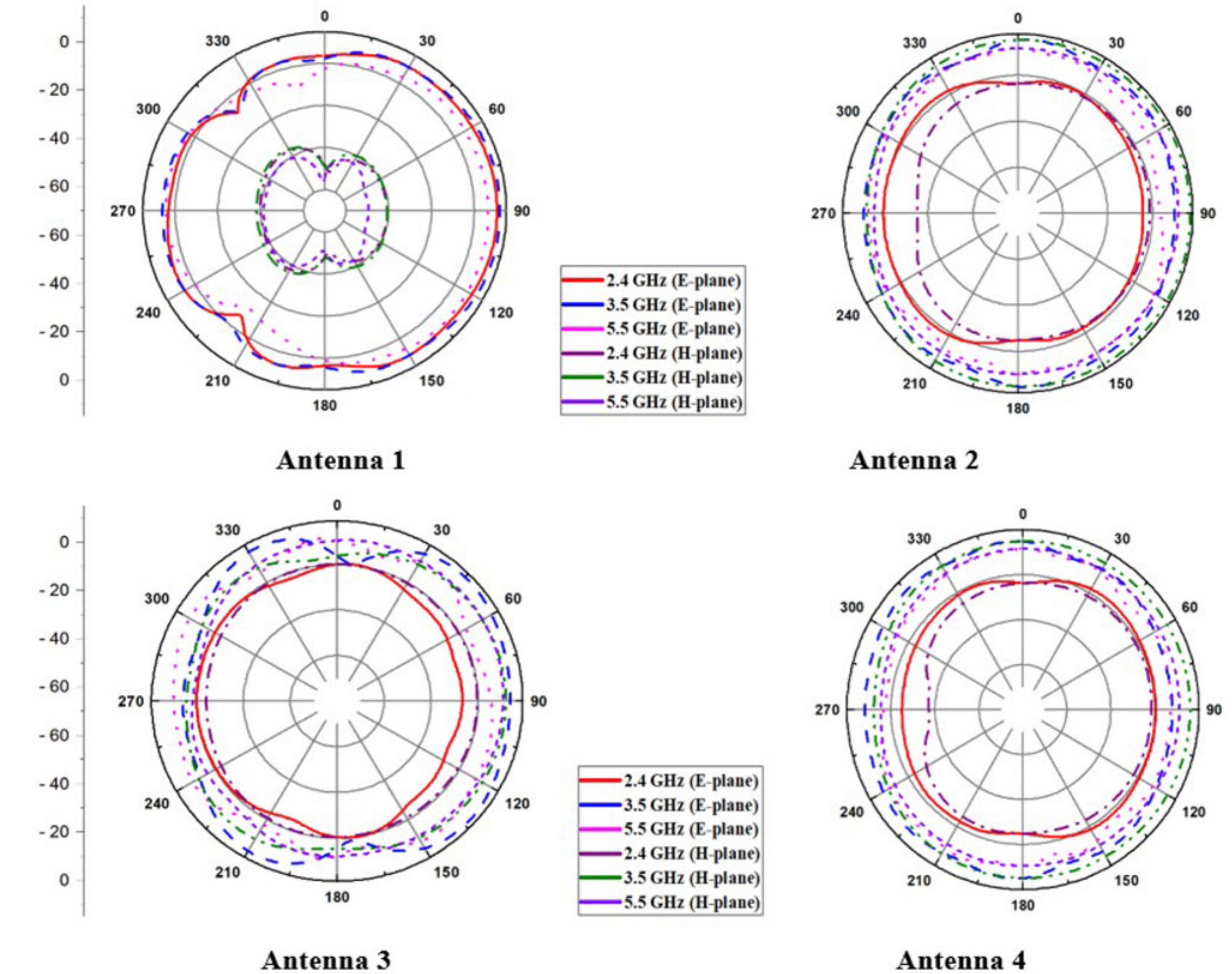

Figure 11. Radiation patterns at 2.4, 3.5, and 5.5 GHz.

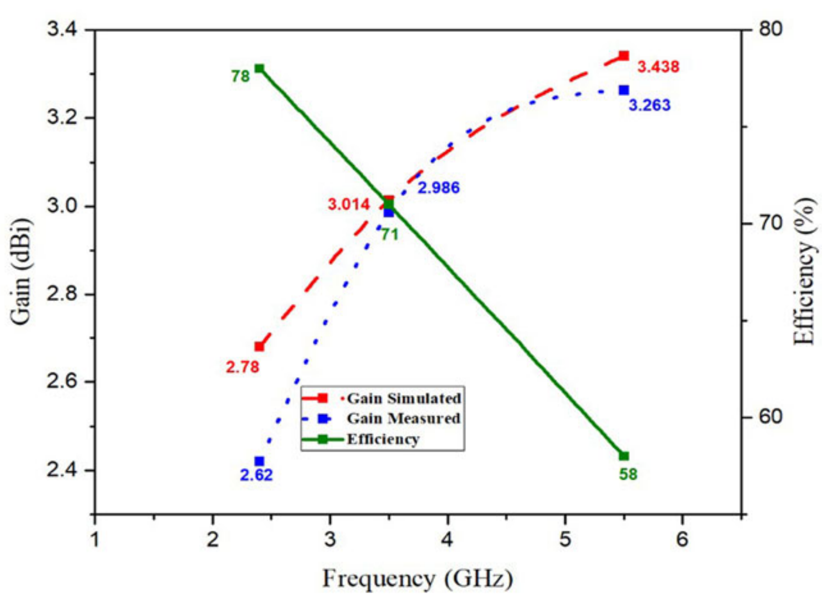

Figure 12. Gain and efficiency of the proposed antenna.

https://doi.org/10.1017/S1759078724000849 Published online by Cambridge University Press

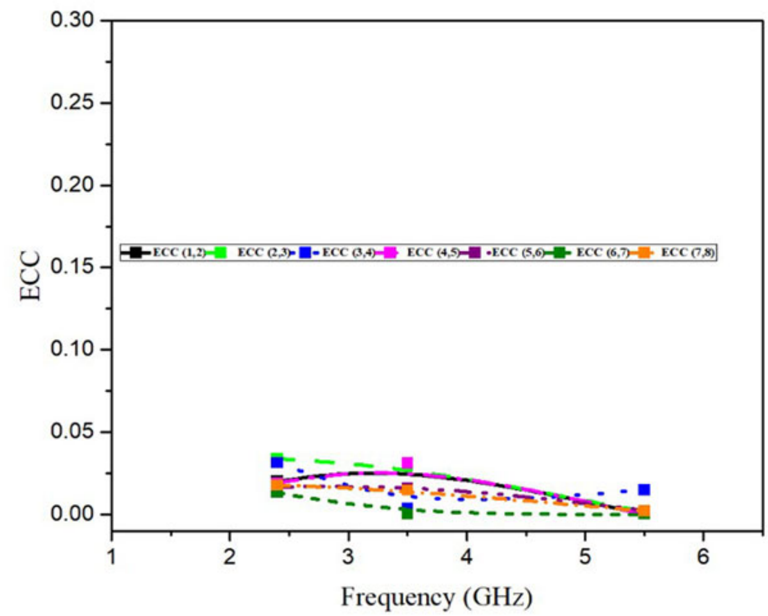

Figure 13. Measured ECC of the antenna.

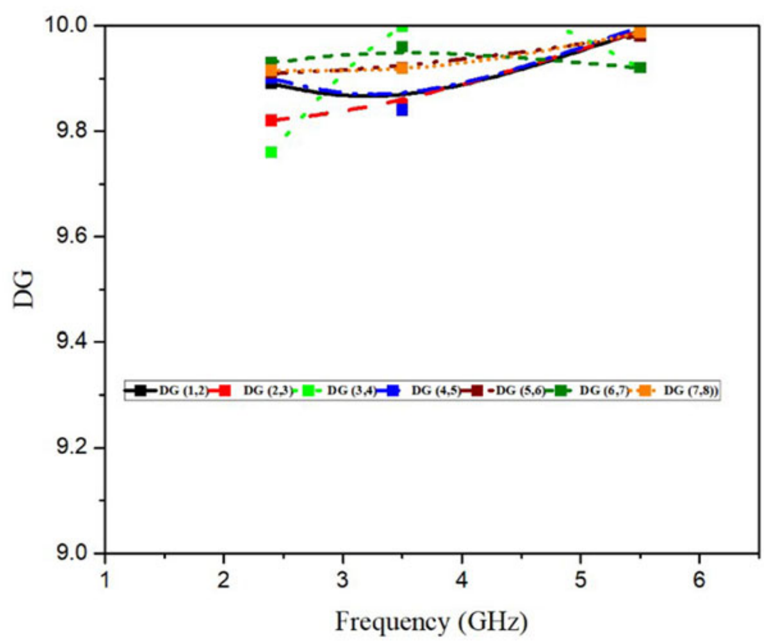

Figure 14. Measured DG of the antenna.

because the substrate used in this work, FR4 with a thickness of 0.8 mm, is widely available. FR4 is inexpensive while comparing with other high-performance substrates, making it a cost-effective choice for production of PCBs. It is a mechanically robust material, providing good support and stability to the antenna design that helps the PCB to withstand physical stress during manufacturing. Also, FR4 is easy to process and handle during PCB manufacturing, including drilling, cutting, and etching.

Figure 9 shows the prototype of the proposed eight-port multiband MIMO antenna whose S-parameter and far-field characteristics are tested using vector network analyzer and anechoic chamber. The measured S-parameters and transmission coefficients are shown in Fig. 10(a) and (b).

Radiation characteristics

The radiation patterns for antennas 1–4 operating in the three bands are given in Fig. 11, which that shows the patterns of the antennas are omnidirectional. The radiation patterns of antennas 5–8 are not presented, as they are nearly the mirror images of antennas 1–4. Figure 12 shows the gain and efficiency of the proposed eight-port multiband MIMO antenna. The obtained gain values are 2.78, 3.014, and 3.438 dBi and

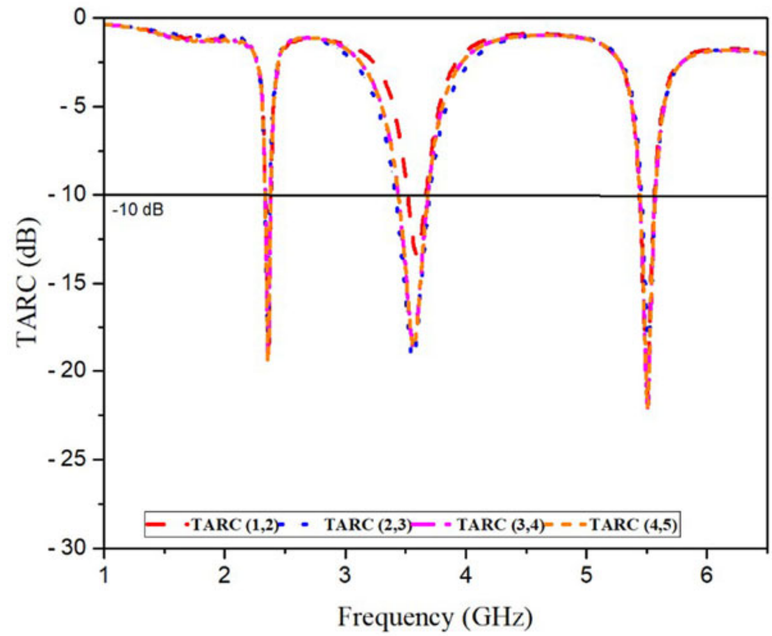

Figure 15. Measured TARC for the proposed MIMO antenna.

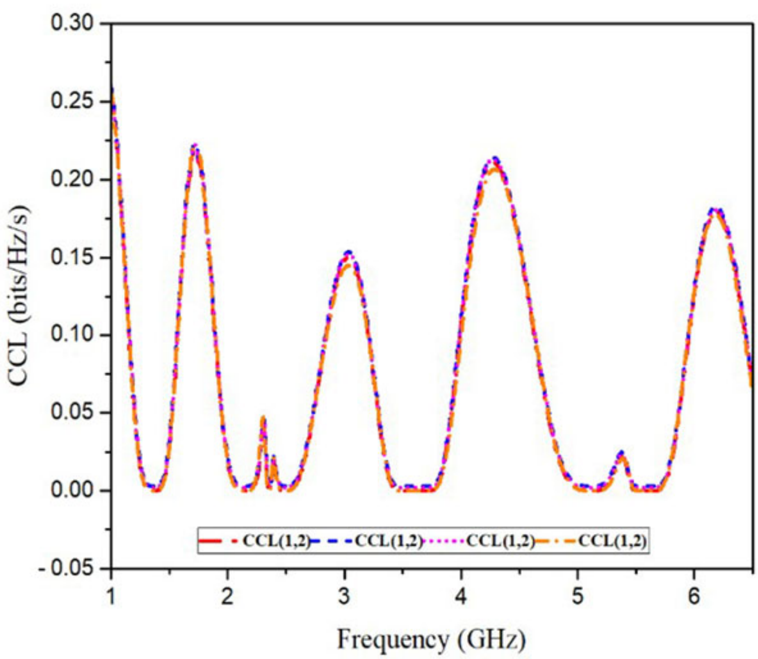

Figure 16. Measured CCL of the antenna.

efficiencies are 78%, 71%, and 58% at 2.4, 3.5, and 5.5 GHz, respectively.

Analysis of the eight-port multiband MIMO antenna

To verify the proposed multiband MIMO characteristics, several metrics such as CCL, ECC, diversity gain (DG), total efficiency, and TARC are studied in this section.

The ECC explains the correlation between the radiating elements. The actual value of ECC is zero but in practical, 0.5 is the acceptable limit. The ECC calculated using equation (4) [18] is less than 0.04, as shown in Fig. 13.

$$\rho_e = \frac{\left| \iint \left[\overrightarrow{F_1}(\theta,\varphi) . \overrightarrow{F_2}(\theta,\varphi) \right] d\Omega \right|^2}{\iint \left| \overrightarrow{F_1}(\theta,\varphi) \right|^2 d\Omega \iint \left| \overrightarrow{F_2}(\theta,\varphi) \right|^2 d\Omega} \tag{4}$$

where F_i denotes far-field radiated by the antenna. (θ, φ) are the angles (elevation, azimuth) and Ω is the solid angle. The measured DG shown in Fig. 14 is mathematically related to ECC as given in equation (5) [14] whose value is >9.98 for the proposed MIMO antenna.

$$DG = 10\sqrt{1 - ECC^2} \tag{5}$$

https://doi.org/10.1017/S1759078724000849 Published online by Cambridge University Press

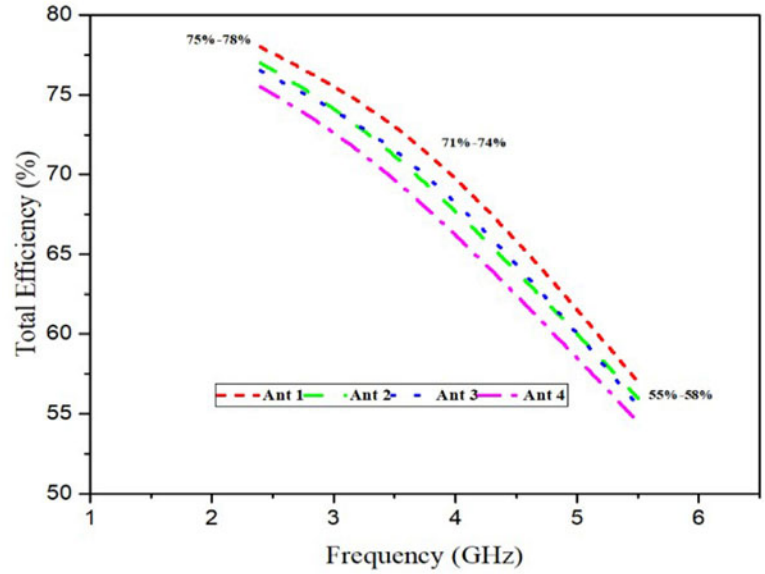

Figure 17. Total efficiency of the proposed antenna.

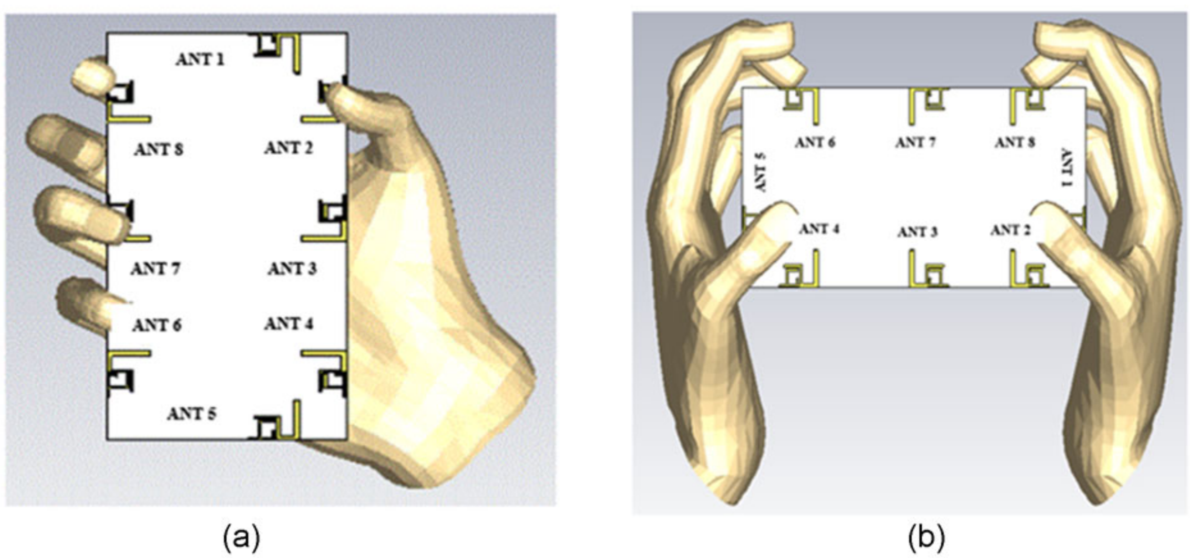

Figure 18. (a), (b). SHM and DHM model of the proposed antenna.

TARC describes the effective operating bandwidth of the antenna system, whose obtained value is less than –10 dB, is shown in Fig. 15, and can be given by equation (6) [17].

$$TARC = \frac{\sqrt{\sum_{i=1}^{N} |b_i|^2}}{\sqrt{\sum_{i=1}^{N} |a_i|^2}} \tag{6}$$

CCL, shown in Fig. 16, compares the performance of the MIMO system with a single antenna system which produces CCL less than 0.25 bits/Hz/s that can be calculated using equation (7) [16, 19]. In Fig. 17, it is observed that the total efficiency of the antennas 1–4 is 55%–78%, and the antennas 5–8 are nearly the mirror image of antennas 1–4.

$$CCL = -log_2 det\,(\theta^{\mu}) \tag{7}$$

$$\theta^{\mu} = \begin{bmatrix} \xi_{11} & \xi_{12} \\ \xi_{21} & \xi_{22} \end{bmatrix} \tag{8}$$

where $\xi_{11} = 1 - \left[|S_{11}|^2 + |S_{12}|^2\right]$; $\xi_{11} = -[S_{11}^{*}S_{12} + S_{21}^{*}S_{12}]$; $\xi_{11} = -[S_{22}^{*}S_{21} + S_{12}^{*}S_{21}]$; $\xi_{11} = 1 - \left[|S_{22}|^2 + |S_{21}|^2\right]$.

Performance analysis using hand-phantom model

In 5G smartphones, where data communication plays a dominant role compared to voice calls, understanding the impact of user hands on antenna performance becomes crucial [20, 21]. This section explains the influence of user's single and double hands on the proposed eight-port multiband MIMO antenna. Through simulations employing a standard hand phantom model, the antenna's behavior is analyzed under single hand mode (SHM) and dual hand mode (DHM) scenarios, as shown in Fig. 18.

https://doi.org/10.1017/S1759078724000849 Published online by Cambridge University Press

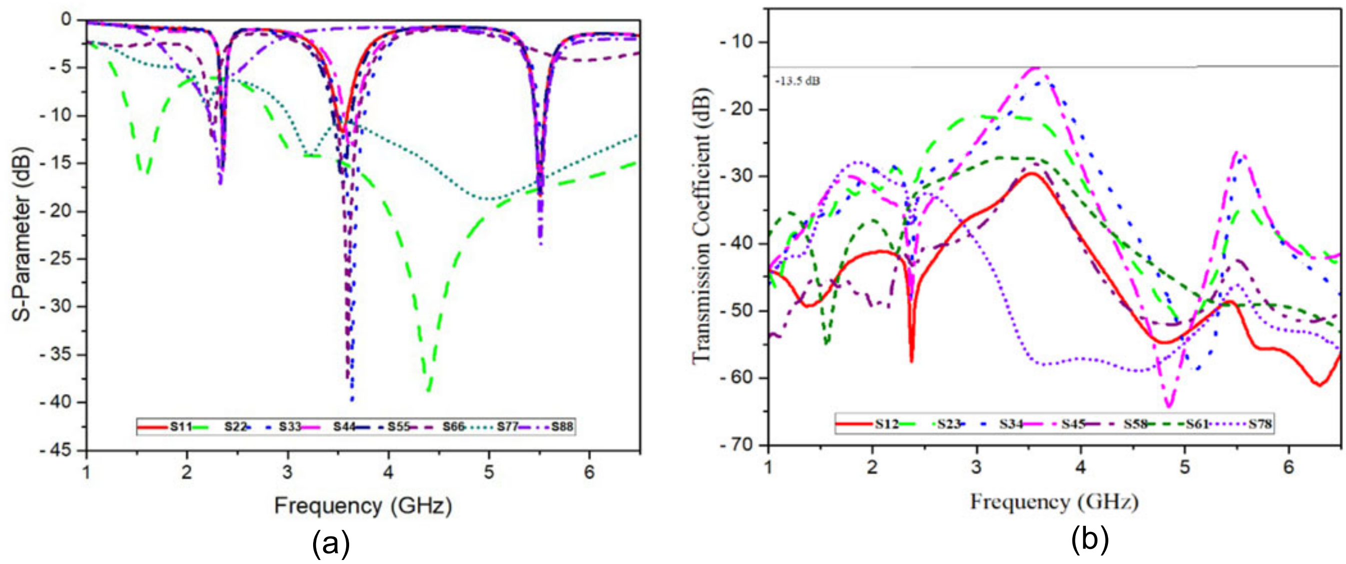

Figure 19. (a), (b). S-parameters of the proposed antenna in SHM.

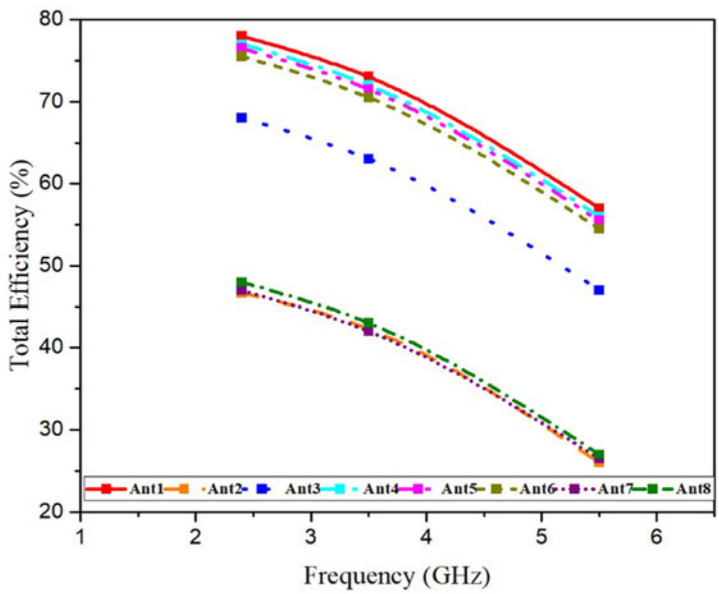

Figure 20. Total efficiency of the proposed antenna in SHM.

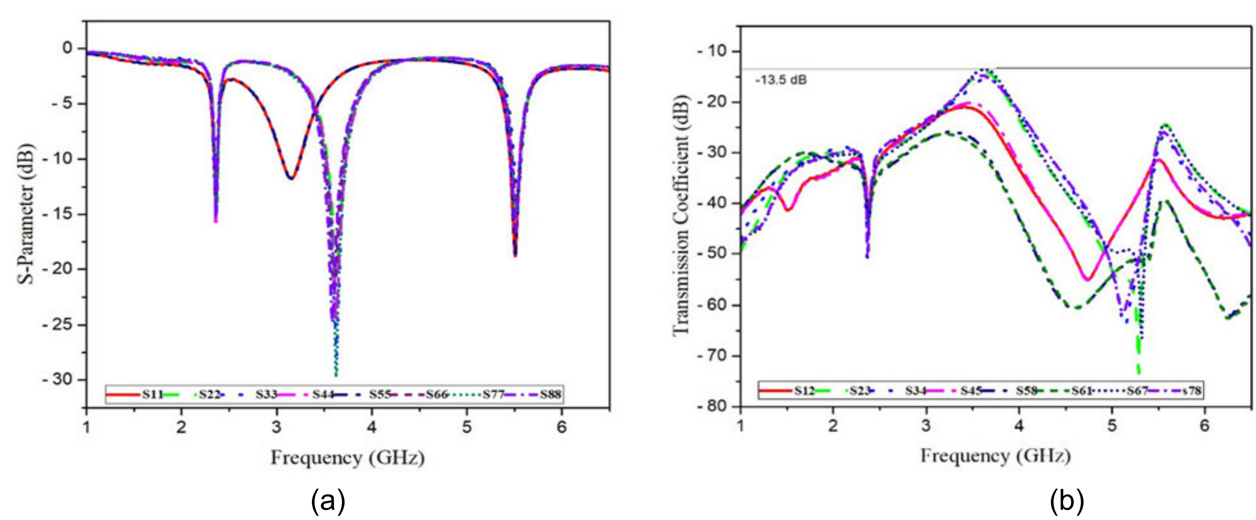

Figure 21. (a), (b). S-parameters of the proposed antenna in DHM.

https://doi.org/10.1017/S1759078724000849 Published online by Cambridge University Press

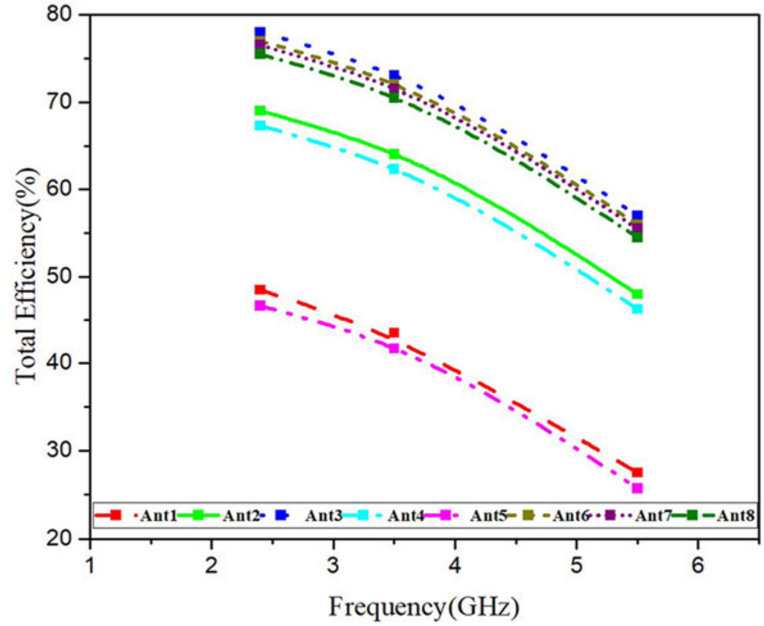

Figure 22. Total efficiency of the proposed antenna in DHM.

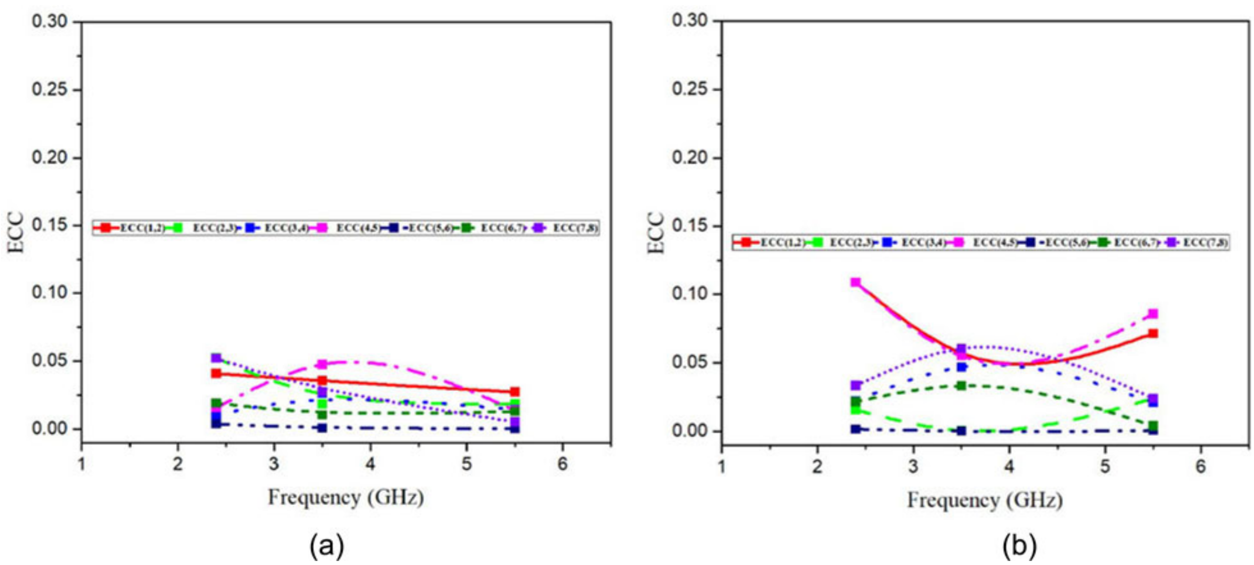

Figure 23. (a), (b). ECC of SHM and DHM of the proposed antenna.

Figure 19 shows the S-parameters for SHM operation. From the figure, it is observed that, in SHM, shifting of frequencies affect the antennas 2, 7, and 8, which have direct contact with the fingers. The efficiency values of antennas 2, 7, and 8 are below 30% due to the absorption of energy in the user's hand, as shown in Fig. 20.

Similarly, the scattering parameters for DHM operations are shown in Fig. 21, which shows that there is a shifting of resonant frequencies in antennas 1 and 5, that have direct contact with the thumb. The scattering parameters of antennas 3 and 6–8 are almost the same, as they are distant from the hand phantom. From Fig. 22, in antennas 1 and 5, the total efficiencies are reduced to 25%. Figure 23 shows that the ECC values of the affected antennas 2, 7, and 8 in SHM and antennas 1 and 5 in DHM gets shifted.

From the analysis of S-parameters, total efficiencies, and ECCs, the proposed MIMO antenna has good performance under SHM and DHM hand-phantom conditions. Table 2 provides the comparison between the hand-held and non-hand-held states of the proposed antenna design.

Table 3 shows the comparison of the proposed antenna with the related published works, which can be explained as,

- The proposed eight-port multiband MIMO antenna has a compact size of $0.132\lambda_0 \times 0.068\lambda_0$ compared to the designs reported in references [6–8, 12, 14, 17, 18].
- The proposed eight-port multiband MIMO antenna covers three operating frequencies at 2.4, 3.5, and 5.5 GHz, unlike reported in references [6–8, 12–15, 17, 18].

Table 2. Comparison of antenna performance under hand-held and non-hand-held states

Measurement state		Isolation (dB)	ECC	Efficiency (%) Antenna 1 2.4 GHz	3.5 GHz	5.5 GHz	Antenna 2 2.4 GHz	3.5 GHz	5.5 GHz	Antenna 5 2.4 GHz	3.5 GHz	5.5 GHz	Antenna 7 2.4 GHz	3.5 GHz	5.5 GHz	Antenna 8 2.4 GHz	3.5 GHz	5.5 GHz
Hand-held	SHM	13.5	0.05	73	74	58	75	71	55	73	74	58	49	46	28	48	45	27
	DHM	13.5	0.1	48	46	27	69	65	49	46	45	25	72	73	56	74	72	57
Non-hand-held		17.5	0.04	73	74	58	75	71	55	73	74	58	72	73	56	74	72	57

Table 3. Comparison of the proposed antenna with other works

Ref., Year	Size of single antenna (λ_0)	Ground size (λ_0)	No. of elements	Frequency (GHz)	Peak gain (dBi)	Efficiency (%)	Isolation (dB)	ECC	DG (dB)	TARC (dB)	CCL (bits/Hz/s)
[6], 2021	0.39 × 0.36	0.15 × 0.15	4	2.3–3.0, 5.4–5.6	1.9, 1.75	–	>14	0.2	>9.8	<−10	–
[7], 2021	0.15 × 0.068	0.08 × 0.068	8	3.4–3.6	3.1	62–76	>12	0.1	>9.3	–	0.37
[8], 2020	0.465 × 0.465	0.2 × 0.15	4	3.1–11	1.52	78	>16	0.16	>9.9	<−10	0.4
[12], 2020	0.16 × 0.19	Common ground	4	2.6, 3.6	4.5	62, 75	>13, >10	0.07	–	<−10	–
[13], 2023	0.08 × 0.07	0.028 × 0.07	8	3.4–3.9, 4.5–5.3	3.4	50, 71	>10	0.18	>9.98	–	–
[14], 2023	0.23 × 0.07	0.077 × 0.825	4	3.3–3.6, 4.4–5	0.6 − 0.8, 0.7 − 2.9	71, 68	>12.8	0.18	–	–	–
[15], 2023	0.44 × 0.44	0.48 × 0.48	4	4.25– 5.13	–	40.3–48.5	>12.5	0.13	>9.5	–	0.4
[16], 2023	0.046 × 0.18	Common ground	8	3.1–3.7, 4.4–4.9, 5.5–6	5.5, 3.5, 3.0	78, 62, 52	>16.2	0.2	>9.0	–	0.4
[17], 2023	0.18 × 0.004	0.132 × 0.55	8	3.3–3.6	–	52.5–63.9	>14.8	0.23	–	<−10	–
[18], 2019	0.035 × 0.25	Common ground	8	3.4–3.6	–	>62	>13.5	0.05	–	–	–
Prop.	0.132 × 0.068	Common ground	8	2.3–2.4, 3.4–3.6, 5.45–5.55	2.7, 3.0, 3.2	78, 71, 58	>17.5	0.04	>9.8	<−10	0.25

- The proposed eight-port multiband MIMO antenna produces improved ECC value of 0.04 than reported in references [6, 8, 12–18].
- The proposed eight-port multiband MIMO antenna produces improved DG value of 9.98 dB than reported in references [6, 7, 15, 16].
- The proposed eight-port multiband MIMO antenna produces improved CCL of 0.25 bits/Hz/s than reported in references [7, 8, 15, 16].
- The proposed eight-port multiband MIMO antenna produces isolation of 17.5 dB unlike in references [6–8, 12–18].

Conclusion

In this work, an eight-port antenna is proposed with small size, which is easy to fabricate and resonates at 2.4, 3.5, and 5.5 GHz. It provides an isolation of >17.5 dB, antenna efficiency (58%–78%) and its parameters such as low ECC < 0.04, high DG > 9.98 dB, improved TARC < −10 dB and CCL < 0.25 bits/Hz/s are observed. The proposed antenna also exhibits good characteristics with hand-phantom. Based on the simulated and measured results, the proposed multiband MIMO antenna is a suitable design for 5G applications.

Competing interests. The author(s) declare no competing interests.

References

1. **Zhang R, Cheng L, Wang S, Lou Y, Gao Y, Wu W and Ng DW** (2024) Integrated sensing and communication with massive MIMO: A unified tensor approach for channel and target parameter estimation. In *IEEE Transactions on Wireless Communications*.
2. **Srivastava K, Kumar S, Kanaujia BK, Dwari S, Choi HC and Kim KW** (2020) Compact eight-port MIMO/diversity antenna with band rejection characteristics. *International Journal of RF and Microwave Computer-Aided Engineering* **30**, e22170.
3. **Wen C, Huang Y, Peng J, Wu J, Zheng G and Zhang Y** (2022) Slow-time FDA-MIMO technique with application to STAP radar. *IEEE Transactions on Aerospace and Electronic Systems* **58**, 74–95.
4. **Singh G, Kumar S, Kanaujia BK and Pandey VK** (2022) Design and implementation of a compact tri-band four-port multiple-input-multiple-output antenna. *International Journal of RF and Microwave Computer-Aided Engineering* **32**, e23218.

5. **Singh G, Kumar S, Kanaujia BK and Pandey VK** (2022) Design and performance analysis of a frequency reconfigurable four-element multiple-input-multiple-output antenna. *AEU - International Journal of Electronics and Communications* **146**, 154118.
6. **Ali H, Ren XC, Bari I, Bashir MA, Hashmi AM, Khan MA, Majid SI, Jan N, Tareen WU and Anjum MR** (2021) Four-port MIMO antenna system for 5G n79 band RF devices. *Electronics* **11**, 35.
7. **Kiani SH, Altaf A, Anjum MR, Afridi S, Arain ZA, Anwar S, Khan S, Alibakhshikenari M, Lalbakhsh A, Khan MA, Abd-Alhameed RA and Ernesto Limiti** (2021) MIMO antenna system for modern 5G handheld devices with healthcare and high rate delivery. *Sensors* **21**, 7415.
8. **Kumar S, Lee GH, Kim DH, Mohyuddin W, Choi HC and Kim KW** (2020) A compact four-port UWB MIMO antenna with connected ground and wide axial ratio bandwidth. *International Journal of Microwave and Wireless Technologies* **12**, 75–85.
9. **Saxena S, Kanaujia BK, Dwari S, Kumar S, Choi HC and Kim KW** (2020) Planar four-port dual circularly polarized MIMO antenna for sub-6 GHz band. *IEEE Access* **8**, 90779–90791.
10. **Ameen M, Ahmad O and Chaudhary RK** (2020) Single split-ring resonator loaded self-decoupled dual-polarized MIMO antenna for mid-band 5G and C-band applications. *AEU - International Journal of Electronics and Communications* **124**, 153336.
11. **Sarkar D and Srivastava KV** (2017) Compact four-element SRR-loaded dual-band MIMO antenna for WLAN/WiMAX/WiFi/4G-LTE and 5G applications. *Electronics Letters* **53**, 1623–1624.
12. **Ojaroudi Parchin N, Al-Yasir YI, Basherlou HJ and Abd-Alhameed RA** (2020) A closely spaced dual-band MIMO patch antenna with reduced mutual coupling for 4G/5G applications. *Progress In Electromagnetics Research C* **101**, 71–80.
13. **Chen Z, Liu Y, Yuan T and Wong H** (2023) A miniaturized MIMO antenna with dual-band for 5G smartphone application. *IEEE Open Journal of Antennas and Propagation* **4**, 111–117.
14. **Hu W, Li Q, Wu H, Chen Z, Wen L, Jiang W and Gao S** (2023) Dual-band antenna pair with high isolation using multiple orthogonal modes for 5G smartphones. *IEEE Transactions on Antennas and Propagation* **71**(2), 1949–1954.
15. **Tian X and Du Z** (2023) Wideband shared-radiator four-element MIMO antenna module for 5G mobile terminals. *IEEE Transactions on Antennas and Propagation* **71**(6), 4799–4811.
16. **Kiani SH, Savci HS, Parchin NO, Rimli H and Hakim B** (2023) Eight element MIMO antenna array with tri-band response for modern smartphones. *IEEE Access* **11**, 44244–44253.
17. **Tian X and Du Z** (2023) Dual-feed shared-radiator metal-frame full-screen mobile phone antenna for GPS and LTE bands with a dual-function capacitor. *IEEE Transactions on Antennas and Propagation* **71**(10), 8314–8319.
18. **Li Y, Sim C-Y-D, Luo Y and Yang G** (2019) High-isolation 3.5 GHz eight-antenna MIMO array using balanced open-slot antenna element for 5G smartphones. *IEEE Transactions on Antennas and Propagation* **67**(6), 3820–3830.
19. **Xiao N, Wang Y, Chen L, Wang G, Wen Y and Li P** (2023) Low-frequency dual-driven magnetoelectric antennas with enhanced transmission efficiency and broad bandwidth. *IEEE Antennas and Wireless Propagation Letters* **22**, 34–38.
20. **Syrytsin I, Pedersen GF and Zhang S** (2024) User effects on mobile phone antennas: Review and potential future solutions. *IEEE Open Journal of Antennas and Propagation* **5**, 5–17.
21. **Zhou D, Sheng M, Bao C, Hao Q, Ji S and Li J** (2024) 6G Non-terrestrial networks-enhanced IoT service coverage: Injecting new vitality into ecological surveillance. *IEEE Network* **38**, 63–71.

A. Vincy Lumina has received her Bachelors degree in Electronics and Communication Engineering from PTR college of Engineering, Madurai and Master's degree in St. Joseph's College of Engineering, Chennai, India in 2015 and 2018 respectively. Currently, she is pursuing her PhD degree in SRM Institute of Science and Technology, Chennai. Her current research interests include Wireless Communications, Antenna Design, Sub–6 GHz, MM-wave applications, 5G applications.

Dr. M. Sangeetha is a senior IEEE member, who received her PhD degree from S.R.M. University, Kattankulathur, and Chennai, India in 2014. She was a gold medalist in her M.Tech degree. Her research interests include Wireless Chaotic Communications, Signal Processing application for Wireless Communication Systems, Internet of Things (IoT) and Machine Learning (ML) algorithms for IoT. Currently she is working as an Associate Professor in the Department of Electronics and Communication Engineering at S.R.M. Institute of Science and Technology (formerly known as SRM University), Kattankulathur, India. She has published 35 International Journal papers, presented 19 International Conference papers and presented 5 papers in National Level Conferences.

Sachin Kumar received the B.Tech. degree in Electronics and Communication Engineering from Uttar Pradesh Technical University, Lucknow, India, in 2009, and the M.Tech. and Ph.D. degrees in Digital Communication and RF & Microwave Engineering from Netaji Subhas University of Technology (East Campus), Delhi, India, in 2011 and 2016, respectively. He was a Post-Doctoral Research Fellow at the College of IT Engineering, Kyungpook National University, South Korea, from 2018 to 2021. He is currently working as Deputy Dean (R&D) and Associate Professor (Research) at Galgotias College of Engineering and Technology, Greater Noida, India. Dr. Kumar has published two books, twelve book chapters, five patents, one hundred and fifty research papers in SCI journals, and over fifty articles in international conferences, and his articles have been cited over 3000 times with an h-index of 30. He is an Associate Editor for the Journal Frontiers in Antennas and Propagation and Franklin Open, Advisory Board Member for the Journal Measurement, Editorial Board Member for the Journal Current Chinese Science, Journal of High-Frequency Communication Technologies, Transactions on Electromagnetic Spectrum, Wearable Technology, and Guest Editor for the International Journal of Antennas and Propagation, Electronics, and Micromachines. He is also a frequent reviewer for more than sixty scientific journals and book publishers. He has given several invited talks at prestigious institutions, and serves as the session chair, organizer, and member of the technical program committee for various national/international conferences, summits, and workshops. His name was featured in the list of "World's Top 2% Scientists" in the 2022, 2021, and 2020 database released by Stanford University, USA and Elsevier. He was a recipient of the Teaching-cum-Research Fellowship from the Government of NCT of Delhi, India, and the Brain Korea 21 Plus Research Fellowship from the National Research Foundation of South Korea. He is a Fellow of the Institute of Electronics and Telecommunication Engineers, India, a Life Member of the Indian Society for Technical Education, and a Member of the Korean Institute of Electromagnetic Engineering and Science.